

**Figure 14.2.5** EPR spectra of  $\text{Mn}^{2+}$ -doped CaO powder: (a) Two-pulse echo-detected EPR spectrum with six strong, narrow  $(|-1/2, m_I\rangle, |1/2, m_I\rangle)$  transitions and weak, broad  $(|\pm 3/2, m_I\rangle, |\pm 1/2, m_I\rangle)$  transitions; (b) Cross section of the PEANUT spectrum at 25 MHz showing the six  $(|-1/2, m_I\rangle, |1/2, m_I\rangle)$  transitions; and (c) Cross section at 4 MHz showing the 10 forbidden  $(|-1/2, m_I\rangle, |1/2, m_I \pm 1\rangle)$  transitions. (Adapted from Ref. [14].)

Quelle: A. Schweiger, G. Jeschke, Principles of Pulse Electron Paramagnetic Resonance, 1st ed., Oxford University Press, Oxford, 2001.

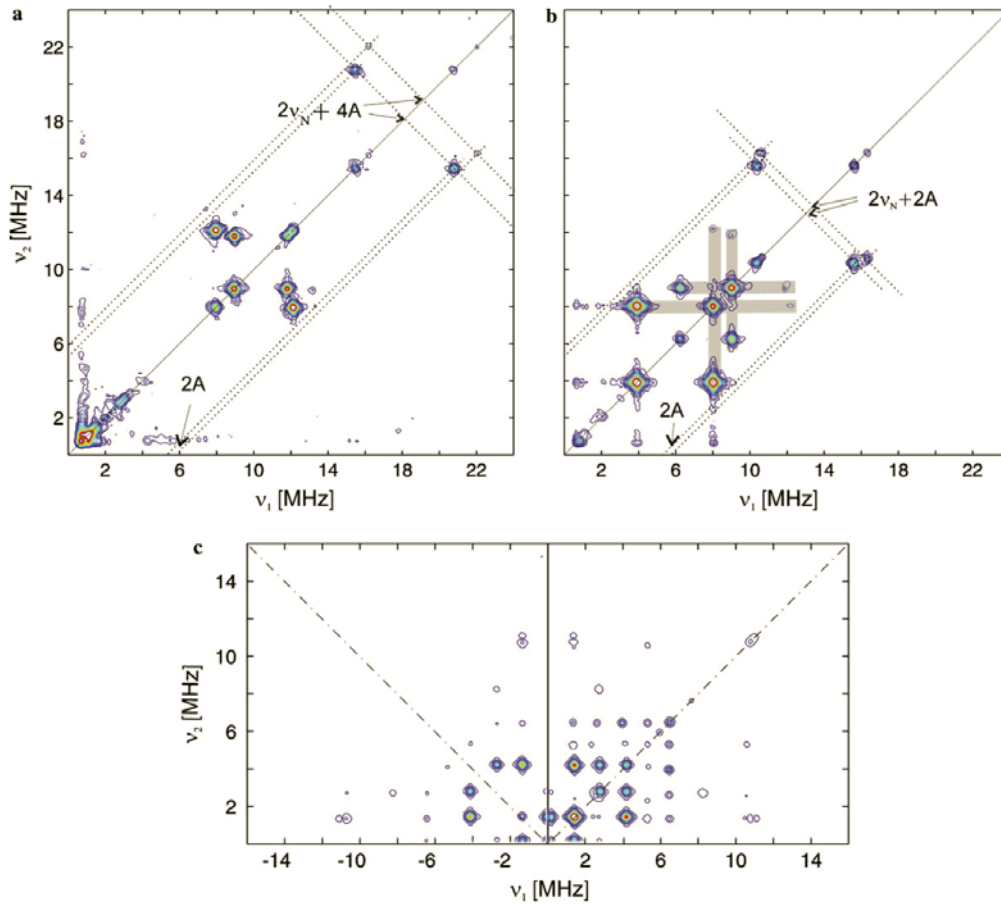


Fig. 5. *Q*-band HYSCORE spectra of  $\text{Mn}(\text{Im})_6$  recorded at one of the electron spin transitions: (a)  $m_S : |-\frac{5}{2}\rangle \rightarrow |-\frac{3}{2}\rangle$ ,  $B_0 = 1183$  mT,  $\tau = 208$  ns; (b)  $m_S : |-\frac{3}{2}\rangle \rightarrow |-\frac{1}{2}\rangle$ ,  $B_0 = 1179$  mT,  $\tau = 208$  ns; (c)  $m_S : |-\frac{1}{2}\rangle \rightarrow |+\frac{1}{2}\rangle$ ,  $B_0 = 1251$  mT,  $\tau = 96$  ns. The magnetic field for all spectra is parallel to the  $z$ -axis of the  $D$  tensor ( $z_D$ ). This orientation is labeled with an asterisk in the rotation patterns shown in Figs. 3, 4 and 8. The nuclear frequencies in correlation patterns a and b can be calculated in a first-order approximation. In this case the hyperfine coupling constant can be directly extracted from the spectrum tracing a line parallel to the diagonal from the dq peaks. The value where this line crosses the abscissa is  $2A$ . If a line perpendicular to the diagonal is drawn, it crosses the diagonal at  $2\nu_N + 4A$  for the  $|-\frac{5}{2}\rangle \rightarrow |-\frac{3}{2}\rangle$  transitions and at  $2\nu_N + 2A$  for  $|-\frac{3}{2}\rangle \rightarrow |-\frac{1}{2}\rangle$ . In spectrum b the crosses formed by the sq peaks (see text) have been highlighted.

Quelle: I. García-Rubio, A. Angerhofer, A. Schweiger, EPR and HYSCORE investigation of the electronic structure of the model complex  $\text{Mn}(\text{imidazole})_6$ : Exploring  $\text{Mn}(\text{II})$ –imidazole binding using single crystals, *J. Magn. Reson.*, 184 (2007) 130-142.

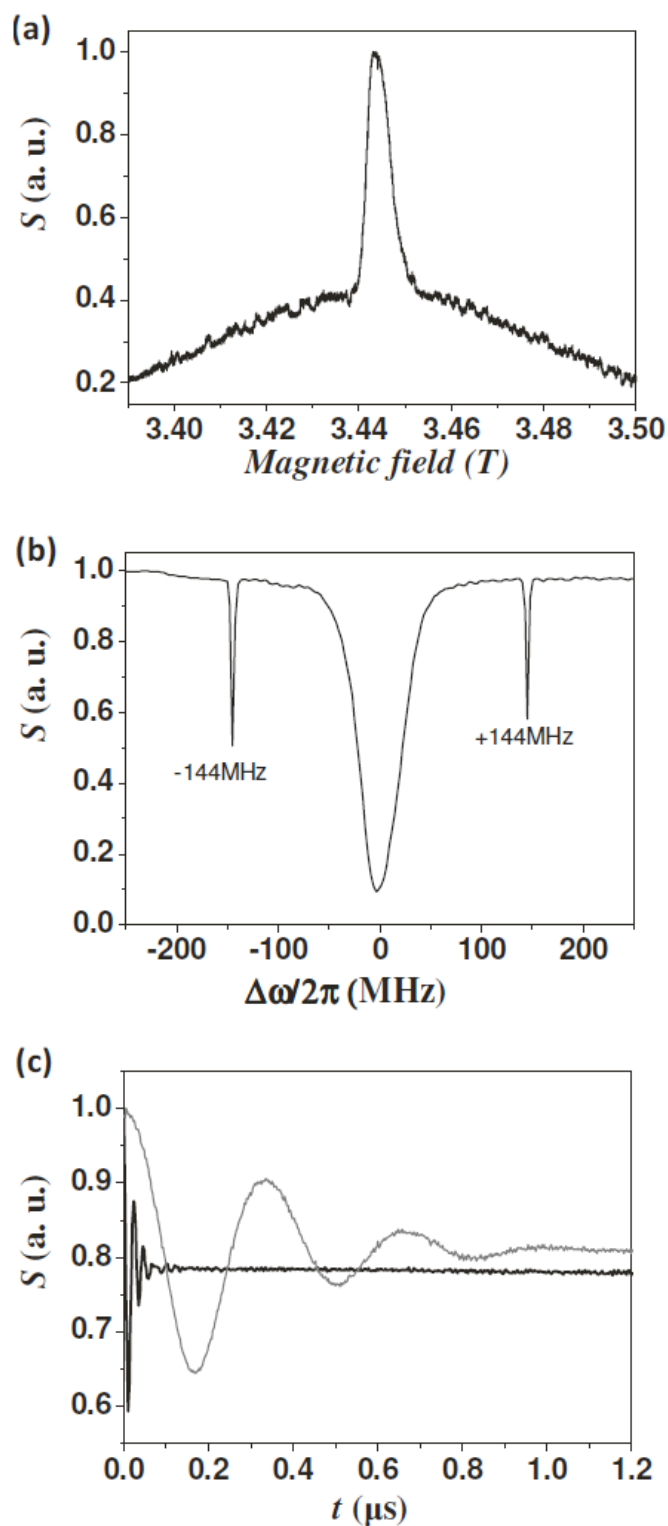


FIG. 2. EPR spectra of (a)  $\text{Gd}^{3+}$  aquo complex recorded at 10 K in water and glycerol solution. (b) ED-NMR spectrum of this solution measured at maximum echo signal. (c) Nutation signal measured at the central frequency (black) and at a frequency off by  $+\omega_n$  (grey).

Quelle: V. Nagarajan, Y. Hovav, A. Feintuch, S. Vega, D. Goldfarb, EPR detected polarization transfer between  $\text{Gd}^{3+}$  and protons at low temperature and 3.3 T: The first step of dynamic nuclear polarization, *J. Chem. Phys.*, 132 (2010) 13.

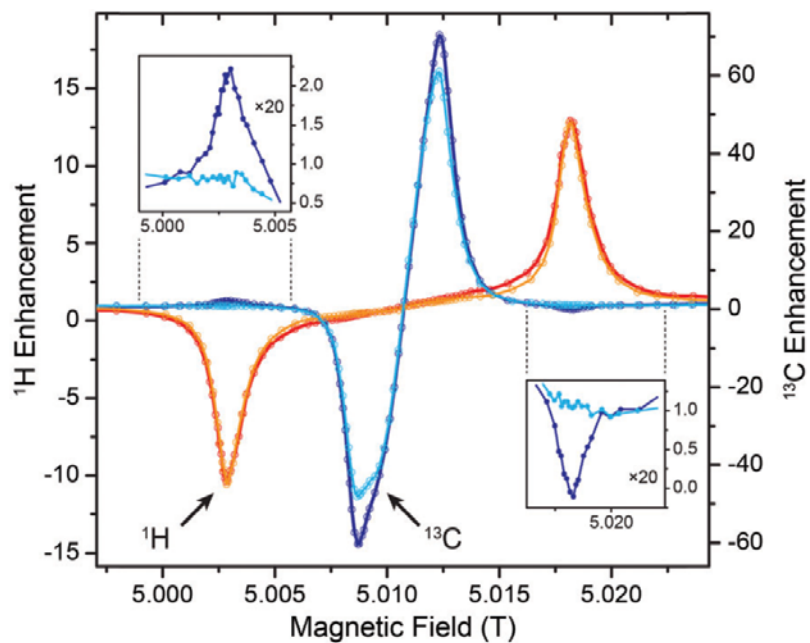
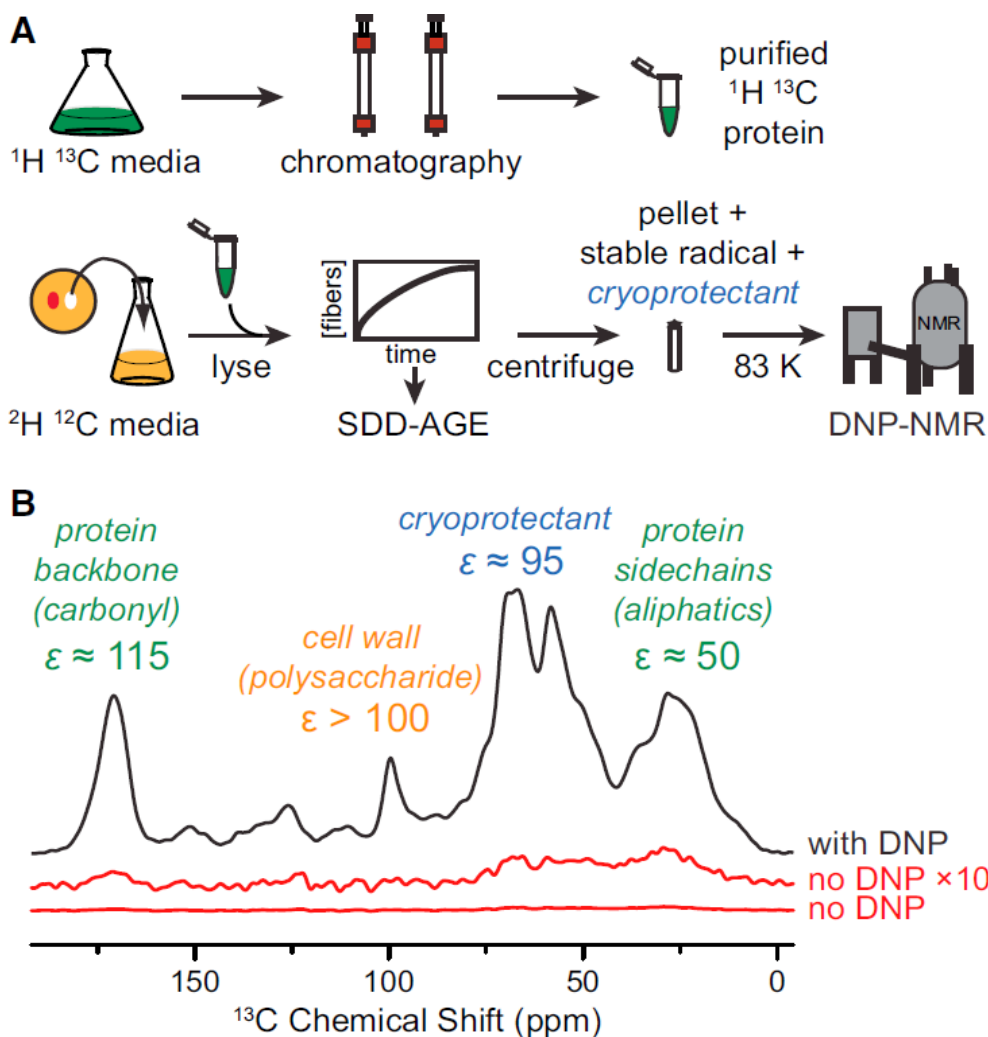


Fig. 5 Proton level dependence of  $^1\text{H}$  (red) and  $^{13}\text{C}$  (blue) DNP at 140 GHz using Gd-DOTA as polarizing agent. Darker profiles are recorded on  $^{13}\text{C}_3$ -glycerol/ $\text{H}_2\text{O}$  (60/40 vol%) as solvent, lighter profiles on  $[\text{D}_8, ^{13}\text{C}_3]$ -glycerol/ $\text{D}_2\text{O}/\text{H}_2\text{O}$  (60/30/10 vol%). The insets show 20-fold vertical magnifications of  $^{13}\text{C}$  enhancements in the respective field region where  $^1\text{H}$  SE condition is matched.

Quelle: M. Kaushik, T. Bahrenberg, T.V. Can, M.A. Caporini, R. Silvers, J. Heiliger, A.A. Smith, H. Schwalbe, R.G. Griffin, B. Corzilius, Gd(III) and Mn(II) complexes for dynamic nuclear polarization: small molecular chelate polarizing agents and applications with site-directed spin labeling of proteins, *Phys. Chem. Chem. Phys.*, 18 (2016) 27205.



**Figure 2. Dynamic Nuclear Polarization Enhances NMR Signals in Cellular Lysates**

(A) Preparation of samples for DNP MAS NMR of proteins at endogenous levels in biological environments. The protein of interest is expressed on isotopically enriched media and purified. The cellular background comes from cells grown on media containing  $D_2O$ . The cells are lysed and the isotopically labeled protein is added exogenously to whole lysate. The mixture is pelleted, the pellet is resuspended in a matrix containing stable radical and cryoprotectant, and the mixture is frozen for analysis by DNP MAS NMR.

(B) One-dimensional  $^{13}C\{^1H\}$  spectra both with (black) and without DNP enhancement by microwaves (red). Dynamic nuclear polarization gave large signal enhancements ( $\epsilon$ ) for uniformly  $^1H\ ^{13}C$ -labeled NM in a deuterated matrix of cellular lysates containing a 60:30:10 (v/v) mixture of  $d_8$ -glycerol: $D_2O$ : $H_2O$  and 10 mM TOTAPOL at 211 MHz/140 GHz with  $\omega/2\pi = 4.3$  kHz and a sample temperature of 83 K.

See also [Figure S1](#).